The high field ordered phase and upper critical field of the filled skutterudite system $Pr(Os_{1-x}Ru_x)_4Sb_{12}$

2008 J. Phys.: Condens. Matter 20 215226

(http://iopscience.iop.org/0953-8984/20/21/215226)

J. Phys.: Condens. Matter **20** (2008) 215226 (8pp) doi:10.1088/0953-8984/20/21/215226

The high field ordered phase and upper critical field of the filled skutterudite system $Pr(Os_{1-x}Ru_x)_4Sb_{12}$

P-C Ho[1,3], N P Butch[1], V S Zapf[1,4], T Yanagisawa[1,5], N A Frederick[1,6], S K Kim[1,7], W M Yuhasz[1,7], M B Maple[1], J B Betts[2] and A H Lacerda[2]

[1] Department of Physics and Institute for Pure and Applied Physical Sciences, University of California, San Diego, La Jolla, CA 92093-0360, USA
[2] National High Magnetic Field Laboratory/LANL, Los Alamos, NM 87545, USA

E-mail: pcho@csufresno.edu

Received 7 January 2008, in final form 28 March 2008
Published 24 April 2008
Online at stacks.iop.org/JPhysCM/20/215226

Abstract
To study the possible competition between unconventional and Bardeen–Cooper–Schrieffer superconductivity in the filled skutterudites $Pr(Os_{1-x}Ru_x)_4Sb_{12}$, the evolution of superconductivity and the high field ordered phase in single-crystal specimens has been investigated by means of electrical resistivity measurements in magnetic fields up to 18 T. Whereas the upper critical field $H_{c2}(T)$ curves have conventional shapes for $x < 0.4$, the $H_{c2}(T)$ curves are nearly linear for $x \gtrsim 0.4$. For all x, $H_{c2}(0)$ matches the calculated value of the orbital critical field. Features in the electrical resistivity associated with the high field ordered phase, observed clearly for $PrOs_4Sb_{12}$, weaken with increasing x and vanish for $x \gtrsim 0.1$.

1. Introduction

Extensive research on the filled skutterudite compound $PrOs_4Sb_{12}$ has been motivated by the unusual physical properties of this compound. Heavy fermion behavior was inferred from the normal state specific heat coefficient γ, the jump in the specific heat ΔC, and the slope of the upper critical field curve $H_{c2}(T)$ near the zero-field superconducting transition temperature T_c [1–3], and was later confirmed by de Haas–van Alphen measurements [4, 5]. No Hebel–Slichter coherence peak was observed in antimony nuclear quadrupole resonance (Sb NQR) measurements, indicating that $PrOs_4Sb_{12}$ does not exhibit BCS superconductivity [6, 7]. An internal magnetic field that breaks time reversal symmetry in the superconducting state of $PrOs_4Sb_{12}$ was observed in μSR measurements [8], which suggests that the superconductivity in $PrOs_4Sb_{12}$ may involve triplet spin pairing of electrons. Upon suppression of the superconductivity by a magnetic field, a high field ordered phase (HFOP) was observed [9], which has been attributed to antiferroquadrupolar ordering [10]. The crystalline electric field (CEF) energy level scheme of the Pr^{3+} ion in $PrOs_4Sb_{12}$ has also been established and consists of a non-magnetic Γ_1 singlet ground state (0 K), a low lying $\Gamma_4^{(2)}$ triplet first excited state (∼7 K), and, at much higher energies, a $\Gamma_4^{(1)}$ triplet excited state (∼130 K), and a Γ_{23} doublet excited state (∼200 K) in T_h symmetry [11–13, 10, 14]. Usually, a Γ_1 non-magnetic singlet ground state should not give rise to heavy fermion behavior. Therefore, it is possible that the heavy electrons and unconventional superconductivity in $PrOs_4Sb_{12}$ result from either magnetic or quadrupole moment excitations involving the Γ_1 singlet ground state and the low lying $\Gamma_4^{(2)}$ first excited state [15, 16, 11].

The analog compound $PrRu_4Sb_{12}$ displays superconductivity below $T_c = 1.1$ K. A coherence peak observed in Sb NQR measurements indicates that $PrRu_4Sb_{12}$ displays BCS superconductivity with an isotropic energy gap

[3] Present address: Department of Physics, California State University, Fresno, CA 93740, USA.
[4] Present address: National High Magnetic Field Laboratory/LANL, Los Alamos, NM 87545, USA.
[5] Present address: Hokkaido University, Sapporo, Japan.
[6] Present address: Independent Project Analysis, Ashburn, VA 20147, USA.
[7] Present address: Department of Physics and Astronomy, Iowa State University, Ames, IA 50011, USA.

$\Delta \approx 1.5k_BT_c$ [6, 7]. Magnetic susceptibility $\chi_{dc}(T)$ and electrical resistivity $\rho(T)$ measurements on $PrRu_4Sb_{12}$ have been interpreted in terms of a Γ_1 singlet ground state and Γ_4 triplet first excited state separated by ~70 K in the simplified O_h crystalline electric field [17, 18]. However, the first excited state of $PrRu_4Sb_{12}$ is presumably a $\Gamma_4^{(2)}$ triplet in T_h symmetry, as found in $PrOs_4Sb_{12}$.

The $Pr(Os_{1-x}Ru_x)_4Sb_{12}$ series of compounds has previously been studied through measurements of $\chi(T)$, $\rho(T)$, specific heat $C(T)$ [19, 20], magnetic penetration depth $\lambda(T)$ [21], and Sb NQR [22], revealing several interesting trends. The superconducting critical temperature T_c is suppressed approximately linearly from the stoichiometric compounds toward $x = 0.6$, suggesting the competition of two types of superconductivity [19]. The CEF splitting between the ground and first excited states increases monotonically and nearly linearly with Ru concentration [20]. The appearance of nodes in the superconducting energy gap for samples with $x \lesssim 0.3$ was implied by Sb NQR spin–lattice relaxation rate [22] and magnetic penetration depth measurements [21], the latter of which indicate the existence of point nodes in the energy gap at low temperatures. Furthermore, strong-coupling superconductivity only appears in a quite narrow region for $0 \leqslant x \lesssim 0.1$ [20, 23]. In order to further investigate the evolution of the unconventional superconductivity, high field ordered phase, and upper critical fields $H_{c2}(x, T)$ in the $Pr(Os_{1-x}Ru_x)_4Sb_{12}$ system, we have performed electrical resistivity measurements on single-crystal specimens with various values of x between 0 and 1 in magnetic fields up to 18 T.

2. Experimental details

The $Pr(Os_{1-x}Ru_x)_4Sb_{12}$ single crystals were prepared by means of an antimony flux growth method as described in [24]. X-ray powder diffraction measurements confirmed that the $Pr(Os_{1-x}Ru_x)_4Sb_{12}$ samples have the cubic $LaFe_4P_{12}$-type structure [25], and the lattice parameter decreases approximately linearly from 9.30 to 9.27 Å as the ruthenium concentration x increases from 0 to 1 [19]. Electrical resistivity $\rho(H, T)$ measurements were performed using a standard four-wire technique in a transverse geometry ($H \perp$ current) with the samples mounted in a ^3He–^4He dilution refrigerator for magnetic fields H between 0 and 18 T. The constant current used was either 100 or 300 μA. High magnetic field experiments (9–18 T) were carried out at the National High Magnetic Field Laboratory at Los Alamos National Laboratory.

3. Results

Displayed in figure 1 is the zero-field superconducting phase diagram, T_c versus x, of $Pr(Os_{1-x}Ru_x)_4Sb_{12}$ from present and previous measurements [19, 20, 26]. The almost linear suppression of T_c from both end member compounds reaches a minimum value of ~0.8 K at $x = 0.6$. The large superconducting transition widths (vertical bars in figure 1) and the significant distribution of T_c values for $x = 0.4$–0.5 apparently arise from an inhomogeneity of Os and Ru

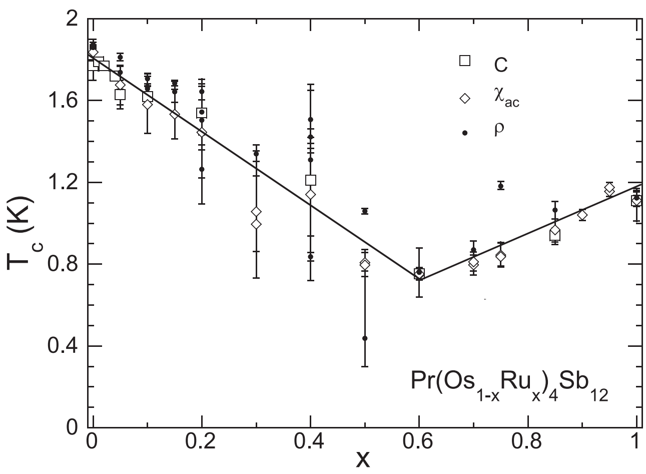

Figure 1. Zero-field superconducting transition temperature T_c versus ruthenium concentration x. Some of the data are from [19, 20, 26]. The two solid lines drawn from $x = 0$ and 1 toward $x = 0.6$ are guides to the eye.

atoms in this composition range despite efforts to overcome this problem by thoroughly mixing elemental powders of Os and Ru with a mortar and pestle.

Figure 2 shows the temperature dependence of the upper critical fields at various ruthenium concentrations; each data point is defined at the 50% drop of $\Delta\rho$ at the superconducting transition. Residual resistivity ratios RRR ($\equiv\rho(300\text{ K})/\rho(2\text{ K})$) of the samples used for the $H_{c2}(T)$ measurements are displayed in figure 3(a). When extrapolated to 0 K, $H_{c2}(0)$ decreases almost monotonically with increasing x (shown in figure 3(b)). For $x \geqslant 0.4$, $H_{c2}(T)$ has an approximately linear T dependence. The kink in the $H_{c2}(T)$ data for $x = 0.2$ at ~0.6 T is due to the occurrence of the peak effect, which may result in lower values in the estimation of $H_{c2}(0)$ and the orbital critical field H^*_{c20}; details will be discussed later. The Ginzburg–Landau coherence length at 0 K, $\xi_{GL}(0)$, can be determined from the formula $H_{c2}(T) = \Phi_0/[2\pi\xi^2_{GL}(T)]$. Figure 3(a) shows the x dependence of $\xi_{GL}(0)$, which varies almost linearly from 122 Å at $x = 0$ to 363 Å at $x = 1$.

The $\rho(T)$ data from 0 to 18 T and the $\rho(H)$ isotherms below 2.1 K in $Pr(Os_{0.95}Ru_{0.05})_4Sb_{12}$ are shown in figures 4(a)–(c). Below 2 T and ~1.7 K, a sharp drop in $\rho(T)$ results from the superconducting transition. In $PrOs_4Sb_{12}$, the high field ordered phase (HFOP) was identified with antiferroquadrupolar order by means of elastic neutron scattering measurements [10]. The HFOP boundaries in $PrOs_4Sb_{12}$ appear as kinks in the $\rho(H)$ isotherms below 1.5 K and a shoulder in the constant-field $\rho(T)$ curves between 4.5 and 15 T [3, 9]. However, these features in the $\rho(T, H)$ data become much smaller when only 5% of ruthenium is substituted into osmium sites. In order to extract the boundary of the HFOP in $Pr(Os_{0.95}Ru_{0.05})_4Sb_{12}$, kinks and peaks in $d\rho/dH$ and $d\rho/dT$ are employed (displayed in figures 5(b) and (c)). The H–T phase diagram of $Pr(Os_{0.95}Ru_{0.05})_4Sb_{12}$ determined in this manner is plotted in figure 5(a). The superconducting phase resides below ~2.3 T, while the HFOP

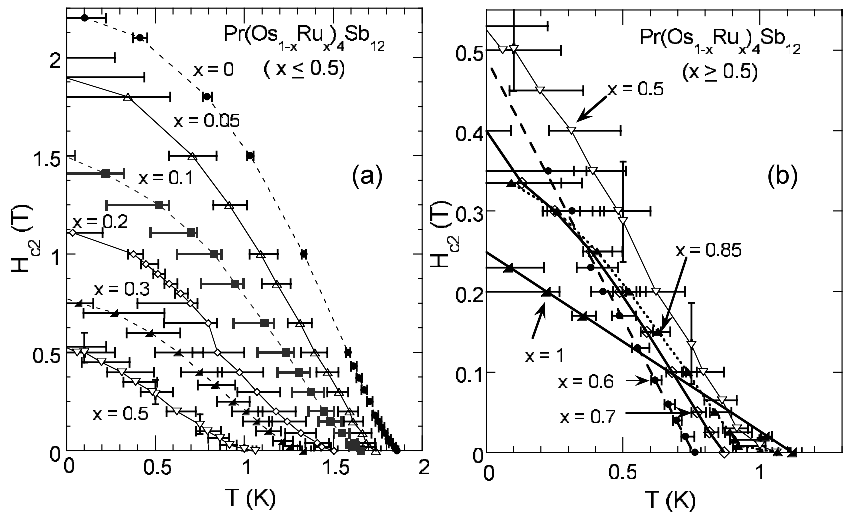

Figure 2. (a) Upper critical field H_{c2} versus temperature T for ruthenium concentrations x between 0 and 0.5. The horizontal or vertical bar associated with each data point represents the transition width, with endpoints corresponding to 10% and 90% of the drop in resistivity due to the superconductivity. (b) H_{c2} versus T for $0.5 \leqslant x \leqslant 1$.

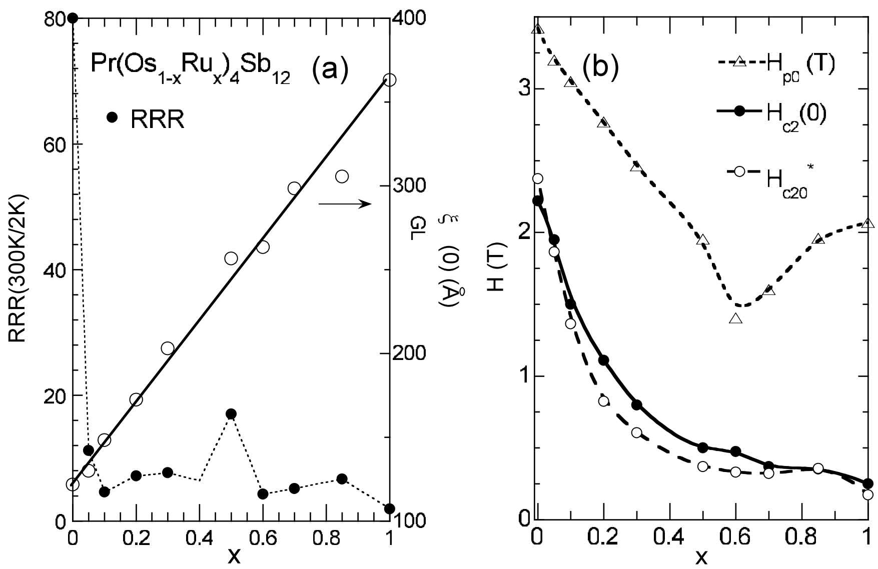

Figure 3. (a) Residual resistivity ratio RRR ($\equiv\rho(300\text{ K})/\rho(2\text{ K})$) (left vertical axis) and zero-kelvin Ginzburg–Landau coherence length $\xi_{GL}(0)$. (b) Zero-kelvin extrapolation of experimentally determined upper critical field $H_{c2}(0)$, estimated orbital critical field H^*_{c20} (equation (1)), and Pauli-limiting field H_{p0} versus ruthenium concentration x.

is located between ∼6 and ∼13 T and below ∼0.6 K. For $x \geqslant 0.1$, no features related to the HFOP were observed in $\rho(T, H)$. Figure 6 summarizes the H–x diagram of the $Pr(Os_{1-x}Ru_x)_4Sb_{12}$ system at $T \sim 0$ K.

Electrical resistivity data $\rho(T, 0\text{ T} \leqslant H \leqslant 18\text{ T})$ and $\rho(H, 0.02\text{ K} \leqslant T \leqslant 2.75\text{ K})$ for $Pr(Os_{0.8}Ru_{0.2})_4Sb_{12}$ are shown in figures 7(a)–(c). Below 2.5 K and 2 T, $\rho(T)$ in the normal state is approximately independent of temperature; above 2 T, there is a slight increase in $\rho(T)$ as T increases (figures 7(a) and (c)). The $\rho(H)$ isotherms below 2.8 K exhibit a broad shoulder at ∼1.7 T; otherwise, the $\rho(H)$ curves have positive linear slopes as H increases (figure 7(c)). No features related to the HFOP are observed in $\rho(H, T)$ in high magnetic fields. A peak effect (PE) appears in the superconducting state above 0.4 T. Selected $\rho(T)$ data in the PE region are shown in figure 7(b). It is interesting that the PE in $\rho(T)$ has an unusual shape with double peaks. The $\rho(T)$ data at 0.8 T, represented by the solid lines in figures 7(a) and (b), serve as a good example that illustrates the structure in $\rho(T)$ associated with the PE. Below the superconducting transition, $\rho(T)$ exhibits a sudden increase at T_{p+} that marks the high T end of the PE, then at T_{p-}, $\rho(T)$ drops to zero, demarcating the low T end of the PE. Two peaks in $\rho(T)$ appear at T_{pk1} and T_{pk2} with a local minimum at T_{pm} where $T_{pk2} < T_{pm} < T_{pk1}$. The current density used in the resistivity measurements was 26.4 μA cm^{-2}. The superconducting H–T phase diagram of $Pr(Os_{0.8}Ru_{0.2})_4Sb_{12}$ is summarized in figure 8.

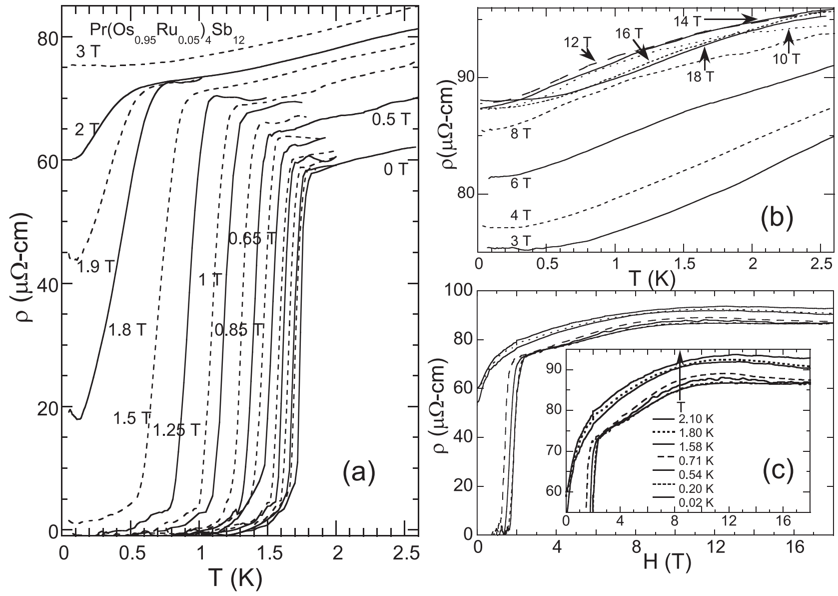

Figure 4. (a) Electrical resistivity ρ versus T in magnetic fields H from 0 to 3 T for $Pr(Os_{0.95}Ru_{0.05})_4Sb_{12}$. The $\rho(T)$ data displayed between 0 and 0.5 T are at $H = 0$, 0.02, 0.04, 0.09, 0.15, 0.2, 0.3, 0.4 T, from right to left. The sharp drop in ρ is due to the superconducting transition. (b) ρ versus T in H from 3 to 18 T. (c) ρ versus H isotherms from 0.02 to 2.10 K.

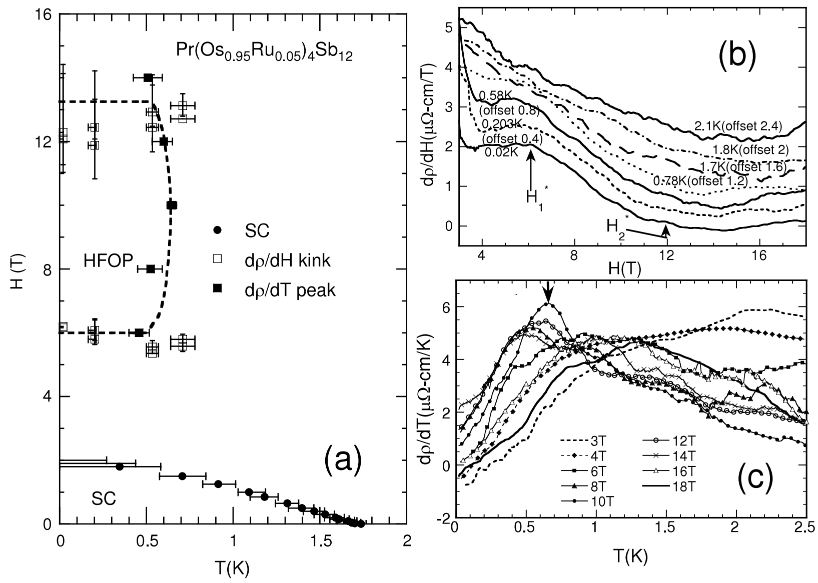

Figure 5. (a) Magnetic field H versus temperature T phase diagram for $Pr(Os_{0.95}Ru_{0.05})_4Sb_{12}$. The phase boundary of the high field ordered phase (HFOP) is determined from $d\rho/dH$ kinks in (b) and $d\rho/dT$ peaks in (c).

4. Discussion

The pronounced minimum of $T_c(x)$ at $x = 0.6$ in the $Pr(Os_{1-x}Ru_x)_4Sb_{12}$ system (figure 1) has been speculated to originate from the competition of the unconventional superconductivity in $PrOs_4Sb_{12}$ and the conventional BCS-type superconductivity in $PrRu_4Sb_{12}$ [19]. However, experimental indications of unconventional superconductivity have been found only at $x < 0.3$. In the following, an alternative explanation is presented. The high T_c of $PrOs_4Sb_{12}$ (1.85 K) relative to that of $LaOs_4Sb_{12}$ (0.74 K) in the $La_{1-x}Pr_xOs_4Sb_{12}$ substitutional series has been ascribed to aspherical Coulomb scattering [11, 27]. The argument is based on a model given by Fulde and co-workers [15, 28], which considers competition between the effects of aspherical Coulomb and exchange scattering between the singlet ground state and the magnetic first excited CEF state. The former interaction serves to enhance T_c, while the latter reduces T_c. Their competition affects the rate of suppression of T_c with substitution of rare earth ions into a superconductor, in which the CEF energy level scheme remains unchanged. Experimental verification of the existence of these two mechanisms was obtained from measurements of T_c and the specific heat jump at T_c versus Pr concentration in

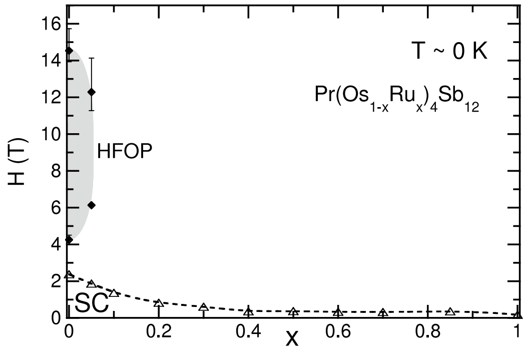

Figure 6. Zero-kelvin H–x phase diagram for $Pr(Os_{1-x}Ru_x)_4Sb_{12}$. The superconducting phase (open triangles) occurs below 2.3 T. The high field ordered phase HFOP (solid diamonds) is located between 4.5 and 15 T and vanishes abruptly above a ruthenium concentration $x = 0.05$. The dashed line and the gray area are guides to the eye.

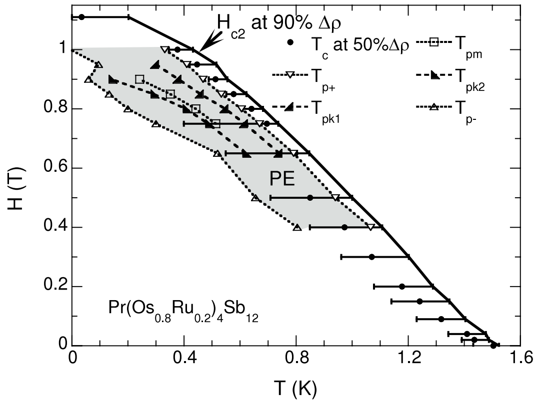

Figure 8. Superconducting H–T phase diagram of $Pr(Os_{0.8}Ru_{0.2})_4Sb_{12}$. The current density is ~ 0.264 A m^{-2}. T_{p+} marks the high T end of the PE, T_{p-} is where $\rho(T)$ drops to zero, demarcating the low T end of the PE. Two peaks in $\rho(T)$ appear at T_{pk1} and T_{pk2} with a local minimum at T_{pm} where $T_{p-} < T_{pk2} < T_{pm} < T_{pk1} < T_{p+}$ (see figure 7(b)).

the $La_{1-x}Pr_xSn_3$ system [29]. A recent study, which has extended the original theoretical framework and applied it to the $La_{1-x}Pr_xOs_4Sb_{12}$ system, confirms that quadrupolar excitations play an important role in the enhancement of T_c in $PrOs_4Sb_{12}$ over that of $LaOs_4Sb_{12}$ [30].

In contrast to the $La_{1-x}Pr_xOs_4Sb_{12}$ series, $Pr(Os_{1-x}Ru_x)_4Sb_{12}$ exhibits a splitting $\Delta_{\Gamma_1\Gamma_4^{(2)}}$ between the singlet ground state and the first excited state of Pr^{3+} that increases monotonically and nearly linearly from $\Delta_{\Gamma_1\Gamma_4^{(2)}} \approx 10$ K at $x = 0$ to $\Delta_{\Gamma_1\Gamma_4^{(2)}} \approx 50$ K at $x = 1$ [19, 20]. Due to the much greater magnitude of $\Delta_{\Gamma_1\Gamma_4^{(2)}}$ in $PrRu_4Sb_{12}$, the low T_c of $PrRu_4Sb_{12}$ (1.1 K) relative to that of $LaRu_4Sb_{12}$ (3.58 K) has been attributed to the aspherical Coulomb scattering being much weaker than the magnetic exchange scattering, which leads to no T_c enhancement [31].

The preceding arguments suggest that in $Pr(Os_{1-x}Ru_x)_4Sb_{12}$, aspherical Coulomb interactions are stronger than magnetic exchange interactions at low x and that the decrease of T_c as x increases can be attributed to two effects: the increase in $\Delta_{\Gamma_1\Gamma_4^{(2)}}$, which weakens both aspherical Coulomb and magnetic exchange interactions, and a decrease in the strength of the aspherical Coulomb effect relative to the magnetic exchange. For $x > 0.6$, the magnetic exchange interaction dominates the aspherical Coulomb interaction and T_c increases with x because the increase of $\Delta_{\Gamma_1\Gamma_4^{(2)}}$ leads to a weakening of the pair-breaking magnetic exchange interaction. Moreover, the linear shape of $H_{c2}(T)$ at the high ruthenium end could result from the temperature dependence of exchange scattering between the CEF ground and first excited states as discussed later. This model can be checked experimentally by measuring the evolution of T_c in the $La(Os_{1-x}Ru_x)_4Sb_{12}$ system. Since the La^{3+} ion does not contain f electrons, there

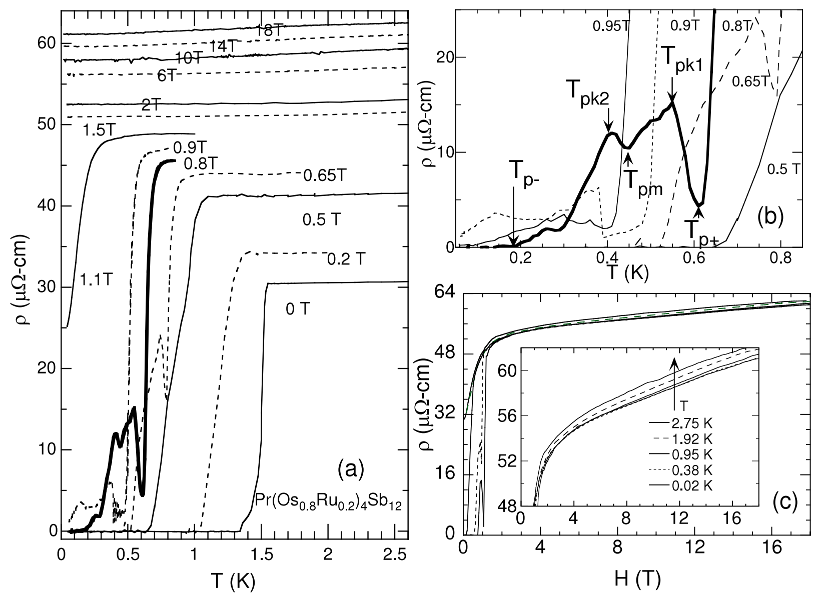

Figure 7. (a) Electrical resistivity ρ versus T for $0\ \mathrm{T} \leqslant H \leqslant 18$ T in $Pr(Os_{0.8}Ru_{0.2})_4Sb_{12}$. (b) Enlarged ρ versus T in the peak effect region. (c) ρ versus H isotherms from 0.02 to 2.75 K.

is no energy level scheme associated with CEF splitting in La^{3+} of $La(Os_{1-x}Ru_x)_4Sb_{12}$. Therefore, there should exist an x_0 for which T_c is equivalent for $La(Os_{1-x0}Ru_{x0})_4Sb_{12}$ and $Pr(Os_{1-x0}Ru_{x0})_4Sb_{12}$, where the aspherical Coulomb scattering and magnetic exchange interactions have equal strength and cancel each other in $Pr(Os_{1-x0}Ru_{x0})_4Sb_{12}$.

Independent of the CEF effects, another possible explanation for the minimum in T_c for $Pr(Os_{1-x}Ru_x)_4Sb_{12}$ is the existence of two-band superconductivity throughout the whole series. Two-band superconductivity in $PrOs_4Sb_{12}$ has been inferred from measurements of thermal conductivity [32]. In $PrOs_4Sb_{12}$, a strong-coupling unconventional superconducting band dominates, while in $PrRu_4Sb_{12}$, a BCS superconducting band dominates, and across the series, superconductivity of one band screens the other and results in the minimum in T_c. Indeed, linearity of $H_{c2}(T)$ in the ruthenium-rich end can also result from two-band superconductivity like that of MgB_2 [33], which will be discussed more later. Recent thermal conductivity measurements on $PrRu_4Sb_{12}$ indicate that two-band superconductivity occurs in this compound as well as $PrOs_4Sb_{12}$ [34].

To simplify analysis of the superconducting upper critical field in $Pr(Os_{1-x}Ru_x)_4Sb_{12}$, the BCS formalism has been followed. Although this rudimentary approach leads only to estimates, it is justified for $x > 0.3$, in which no nodes have been observed in the superconducting energy gap [22, 21], and for clarity has been extended to all values of x. The Pauli-paramagnetism-limited upper critical field at 0 K follows the relation $H_{p0} = 1.84\ \mathrm{T\,K^{-1}} \times T_c$ [35, 36]. From the initial slope of H_{c2} and zero-field T_c, the orbital critical field can be calculated from equation (1):

$$H^*_{c20} \approx 0.693 T_c \left(\left. \frac{\mathrm{d}H_{c2}}{\mathrm{d}T} \right|_{T_c} \right). \qquad (1)$$

Note that 0.693 is the value for the dirty limit; however, in the clean limit, the value is 0.705, which is less than 1% different, so we use the value of 0.693 for estimation. The x dependences of H_{p0} (open triangles) and H^*_{c20} (open circles) are shown in figure 3(b), in comparison with the $H_{c2}(0)$ experimentally extrapolated from $H_{c2}(T)$ at each concentration. The extrapolated value of $H_{c2}(0)$ lies much lower than H_{p0} and is very close to H^*_{c20}, indicating that the superconducting pair-breaking effect primarily comes from the orbital motion of electrons in this substituted system.

Near T_c, ξ_{GL} and the BCS coherence length ξ_0 are related as [37]

$$\xi_{GL}(T) = \begin{cases} 0.74\, \dfrac{\xi_0}{(1 - T/T_c)} & \text{clean limit} \quad (\xi_0/\ell \ll 1), \\ 0.855 \dfrac{(\xi_0 \ell)^{1/2}}{(1 - T/T_c)} & \text{dirty limit} \quad (\xi_0/\ell \gg 1), \end{cases} \qquad (2)$$

where ℓ is the mean free path. Therefore, at $T = 0$ K

$$H^*_{c20} = \begin{cases} \dfrac{\Phi_0}{1.1\pi \xi_0^2} & \text{clean limit,} \\ \dfrac{\Phi_0}{1.46\pi \xi_0 \ell} & \text{dirty limit.} \end{cases} \qquad (3)$$

The mean free path ℓ can be estimated using the Drude model with a simplified isotropic Fermi surface $\rho_0 = m^*/(ne^2\tau) = m^* \upsilon_F/(ne^2\ell) = \hbar k_F/(ne^2\ell)$, where ρ_0 is the measured residual resistivity, m^* is the electron effective mass, υ_F is the Fermi velocity, n is the density of the charge carriers, which is approximated by two holes per unit cell for all concentrations, and $k_F = (3\pi^2 n)^{1/3}$ is the Fermi momentum. However, due to the small size of the samples, it is difficult to determine the geometrical factor accurately so as to obtain reliable estimates of ℓ for all x. From the values of the RRR (300 K/2 K; figure 3(a)) and the assumption that room temperature resistivities are roughly the same for all samples, we infer that $PrOs_4Sb_{12}$ is in the clean limit, $PrRu_4Sb_{12}$ in the dirty limit, and the rest of the samples are in the intermediate regime with ξ_0/ℓ ranging from 0.5 to 6, where equation (3) is not applicable. Therefore, from $\xi_0 = 0.18\hbar\upsilon_F/(k_B T_c)$ and $\hbar k_F = m^*_{sc}\upsilon_F$, the values of the superconducting electron effective mass m^*_{sc} of $PrOs_4Sb_{12}$ and $PrRu_4Sb_{12}$ are $\sim 23\ m_e$ and $\sim 5\ m_e$, respectively.

The linear T dependence of $H_{c2}(T)$ for $x \geqslant 0.4$ is quite peculiar (figure 2(b)). For a conventional BCS superconductor, the upper critical field $H_{c2}(T)$ curve has a convex shape and is linear near the zero-field T_c and saturates at low temperature T with zero slope as $T \to 0$. For $Pr(Os_{1-x}Ru_x)_4Sb_{12}$, the convex $H_{c2}(T)$ occurs for unconventional superconductivity, while the approximately linear $H_{c2}(T)$ curve occurs near the region of conventional superconductivity. Two possible scenarios for a BCS superconductor that may result in a linear $H_{c2}(T)$ curve are (I) by means of CEF effects and (II) via two-band superconductivity. In scenario (I), two competing pair-breaking effects play dominant roles in a BCS superconductor with a fixed amount of rare earth impurities with a singlet ground state upon the application of a magnetic field: one simply is the applied magnetic field and the other comes from the inelastic exchange scattering between the CEF ground and first excited states of the rare earth ion. Due to the decrease of the inelastic scattering between the CEF ground and first excited states as T decreases, this pair-breaking effect decreases and the curve of H_{c2} straightens in the low temperature region [38]. Such behavior has been found previously in $H_{c2}(T)$ of $(La_{1-x}Pr_x)_3In$ and $(La_{1-x}Tb_x)Al_2$ [39, 40]. In scenario (II), because there are two different $H_{c2}(T)$ curves for two-band superconductivity, the resulting H_{c2} could have a nearly linear T dependence. The archetype of a two-band superconductor MgB_2 has a quite linear $H_{c2}(T)$ curve [33, 41]. It is unclear whether this linear behavior of $H_{c2}(T)$ results from CEF effects, because such linearity is also observed in $LaOs_4Sb_{12}$ [42], which is a BCS superconductor without the complications of the CEF effects. However, currently there is no experimental evidence indicating two-band superconductivity in $LaOs_4Sb_{12}$, although evidence does exist for $PrRu_4Sb_{12}$, as noted earlier [34]. Further thermal conductivity measurements on $LaOs_4Sb_{12}$ could clarify this issue.

Regarding the disappearance of the HFOP above $x = 0.1$ in $Pr(Os_{1-x}Ru_x)_4Sb_{12}$, a similar trend also appears in previously published specific heat studies [20]. The x dependence of the superconducting specific heat jump divided by T_c, $\Delta C/T_c$, shows a sharp drop from $x = 0$ to 0.1 (a reduction in size of ~7 times), and for $x \geqslant 0.1$, $\Delta C/T_c$ remains approximately constant. An interesting correlation is also observed in recent μSR studies: the spontaneous moment in the superconducting state vanishes by $x \sim 0.2$ [23]. The connection between these three experiments strongly suggests that the large γ enhancement and unconventional nature of the superconducting state in $PrOs_4Sb_{12}$ are related to the existence of strong quadrupolar interactions.

The double-peak structure in the PE has been previously observed in a critical current density study on $PrOs_4Sb_{12}$ by Sato and co-workers [43]. They attributed the PE in $PrOs_4Sb_{12}$ to two superconducting phases with different order parameter symmetries (twofold and fourfold) found in thermal conductivity measurements [44]. The PE usually occurs in very clean samples where the pinning of the flux line lattice is weak and rarely occurs in chemically substituted samples where pinning due to disorder is usually very strong. As a rough indication of disorder, the value of the residual resistivity ratio RRR(300 K/2 K) of the $Pr(Os_{0.8}Ru_{0.2})_4Sb_{12}$ sample is rather low: 7.2. Thus the mechanism causing the PE in $Pr(Os_{0.8}Ru_{0.2})_4Sb_{12}$ is not currently understood. However, the previous measurements of the magnetic penetration depth suggested that point nodes in the superconducting energy gap disappear at the concentration $x \sim 0.3$ in $Pr(Os_{1-x}Ru_x)_4Sb_{12}$ [21]. An anomalous PE at $x = 0.2$ could result from the proximity to the crossover of two types of superconductivity. More experiments are needed to clarify this situation.

5. Summary

Competition between unconventional and conventional superconductivity in $Pr(Os_{1-x}Ru_x)_4Sb_{12}$ was observed throughout the Ru substituent dependence of T_c and the curvature of $H_{c2}(T)$. On the basis of this resistive upper critical field study, the orbital motion of electrons is the main factor that limits $H_{c2}(T)$ in $Pr(Os_{1-x}Ru_x)_4Sb_{12}$. Possible explanations for the minimum of T_c and the shape of the $H_{c2}(T)$ curves, including CEF effects and two-band superconductivity, are discussed. A simplified analysis based on the BCS theory indicates that $PrOs_4Sb_{12}$ is in the clean limit, $PrRu_4Sb_{12}$ is in the dirty limit, and the rest of the samples are in the intermediate regime. The estimated effective masses of the superconducting electrons are ~23 m_e for $PrOs_4Sb_{12}$ and ~5 m_e for $PrRu_4Sb_{12}$, respectively.

The rapid suppression of the HFOP, $\Delta C/T_c$, and the spontaneous moment in the superconducting state for $x \sim 0.2$ in $Pr(Os_{1-x}Ru_x)_4Sb_{12}$ suggest that electric quadrupole interactions may be involved in the formation of the heavy fermion state and unconventional superconductivity in $PrOs_4Sb_{12}$. The peak effect with a double-peak structure was observed in the $Pr(Os_{0.8}Ru_{0.2})_4Sb_{12}$ sample with a low RRR value of ~7.2, although the mechanism behind it is unclear.

Acknowledgments

We thank A Thrall, who was a summer REU student in 2003, for assistance with the growth of some of the samples of $Pr(Os_{1-x}Ru_x)_4Sb_{12}$. We thank R E Baumbach and B J Taylor for helpful discussions. Sample growth was supported by the US Department of Energy under Grant No. DE-FG02-04ER46105 and measurements at UCSD were supported by the National Science Foundation under Grant No. DMR-0335173. The work at the NHMFL Pulsed Field Facility (Los Alamos National Laboratory) was performed under the auspices of the NSF, the State of Florida and the US Department of Energy.

References

[1] Maple M B, Ho P-C, Zapf V S, Frederick N A, Bauer E D, Yuhasz W M, Woodward F M and Lynn J W 2002 *J. Phys. Soc. Japan* **71** 23
[2] Bauer E D, Frederick N A, Ho P-C, Zapf V S and Maple M B 2002 *Phys. Rev.* B **65** 100506R
[3] Ho P-C, Zapf V S, Bauer E D, Frederick N A, Maple M B, Giester G, Rogl P, Berger S T, Paul C H and Bauer E 2002 *Int. J. Mod. Phys.* B **16** 3008
[4] Sugawara H, Osaki S, Saha S R, Aoki Y, Sato H, Inada Y, Shishido H, Settai R, Onuki Y, Harima H and Oikawa K 2002 *Phys. Rev.* B **66** 220504R
[5] Sugawara H, Osaki S, Saha S R, Aoki Y, Sato H, Inada Y, Shishido H, Settai R and Onuki Y 2003 *Acta Phys. Pol.* B **34** 1125
[6] Yogi M, Kotegawa H, Imamura Y, Zheng G Q, Kitaoka Y, Sugawara H and Sato H 2003 *Phys. Rev.* B **67** 180501 (*Preprint* cond-mat/0303569)
[7] Kotegawa H, Yogi M, Imamura Y, Kawasaki Y, Zheng G Q, Kitaoka Y, Ohsaki S, Sugawara H, Aoki Y and Sato H 2003 *Phys. Rev. Lett.* **90** 027001
[8] Aoki Y, Tsuchiya A, Kanayama T, Saha S R, Sugawara H, Sato H, Higemoto W, Koda A, Ohishi K, Nishiyama K and Kadono R 2003 *Phys. Rev. Lett.* **91** 067003
[9] Ho P-C, Zapf V S, Frederick N A, Bauer E D, Do T D, Maple M B, Christianson A D and Lacerda A H 2003 *Phys. Rev.* B **67** 180508(R)
[10] Kohgi M, Iwasa M N K, Metoki N, Araki S, Bernhoeft N, Mignot J-M, Gukasov A, Sato H, Aoki Y and Sugawara H 2003 *J. Phys. Soc. Japan* **72** 1002
[11] Goremychkin E A, Osborn R, Bauer E D, Maple M B, Frederick N A, Yuhasz W M, Woodward F M and Lynn J W 2004 *Phys. Rev. Lett.* **93** 157003
[12] Aoki Y, Namiki T, Ohsaki S, Saha S R, Sugawara H and Sato H 2002 *J. Phys. Soc. Japan* **71** 2098
[13] Tayama T, Sakakibara T, Sugawara H, Aoki Y and Sato H 2003 *J. Phys. Soc. Japan* **72** 1516
[14] Rotundu C R, Tsujii H, Takano Y, Andraka B, Sugawara H, Aoki Y and Sato H 2004 *Phys. Rev. Lett.* **92** 037203/1
[15] Fulde P, Hirst L L and Luther A 1970 *Z. Phys.* **230** 155
[16] Fulde P and Jensen J 1983 *Phys. Rev.* B **27** 4085
[17] Takeda N and Ishikawa M 2000 *J. Phys. Soc. Japan* **69** 868
[18] Abe K, Sato H, Matsuda T D, Namiki T, Sugawara H and Aoki Y 2002 *J. Phys.: Condens. Matter* **14** 11757
[19] Frederick N A, Do T D, Ho P-C, Butch N P, Zapf V S and Maple M B 2004 *Phys. Rev.* B **69** 024523
[20] Frederick N A, Sayles T A and Maple M B 2005 *Phys. Rev.* B **71** 064508
[21] Chia E E M, Vandervelde D, Salamon M B, Kikuchi D, Sugawara H and Sato H 2005 *J. Phys.: Condens. Matter* **17** L303
[22] Nishiyama M, Kato T, Sugawara H, Kikuchi D, Sato H, Harima H and Zheng G-Q 2006 *Physica* B **378–380** 192
[23] Shu L, MacLaughlin D E, Aoki Y, Tunashima Y, Yonezawa Y, Sanada S, Kikuchi D, Sato H, Heffner R H, Higemoto W, Ohishi K, Ito T U, Bernal O O, Hillier A D, Kadono R, Koda A, Ishida K, Sugawara H, Frederick N A,

Yuhasz W M, Sayles T A, Yanagisawa T and Maple M B 2007 *Phys. Rev.* B **76** 014527

[24] Bauer E D, Ślebarski A, Freeman E J, Sirvent C and Maple M B 2001 *J. Phys.: Condens. Matter* **13** 4495

[25] Jeitschko W and Braun D 1977 *Acta Crystallogr.* B **33** 3401

[26] Frederick N A, Sayles T A, Kim S K and Maple M B 2007 *J. Low Temp. Phys.* **147** 321–33

[27] Rotundu C R, Kumar P and Andraka B 2006 *Phys. Rev.* B **73** 014515

[28] Keller J and Fulde P 1971 *J. Low Temp. Phys.* **4** 289

[29] McCallum R W, Fertig W A, Luengo C A, Maple M B, Brucher E, Maita J P, Sweedler A R, Mattrix L, Fulde P and Keller J 1975 *Phys. Rev. Lett.* **34** 1620

[30] Chang J, Eremin I, Thalmeier P and Fulde P 2007 *Preprint* cond-mat/0709.3849

[31] Adroja D T, Park J-G, Goremychkin E A, Takeda N, Ishikawa M, McEwen K A, Osborn R, Hillier A D and Rainford B D 2005 *Physica* B **359–361** 983

[32] Seyfarth G, Brison J P, Measson M-A, Flouquet J, Izawa K, Matsuda Y, Sugawara H and Sato H 2005 *Phys. Rev. Lett.* **95** 107004

[33] Muller K-H, Fuchs G, Handstein A, Nenkov K, Narozhnyi V N and Eckert D 2001 *J. Alloys Compounds* **322** L10

[34] Hill R W, Li S, Maple M B and Taillefer L 2007 *Preprint* cond-mat/0709.4265

[35] Decroux M and Fischer Ø 1982 *Superconductivity in Ternary Compounds II* (*Topics in Current Physics* vol 34) ed M B Maple and Ø Fischer (Berlin: Springer) chapter 3

[36] Hake R R 1967 *Appl. Phys. Lett.* **10** 189

[37] Tinkham M 1983 *Introduction to Superconductivity* 1st edn (New York: McGraw-Hill) chapter 4

[38] Keller J and Fulde P 1973 *J. Low Temp. Phys.* **12** 63

[39] Heiniger F, Bucher E, Maita J P and Longinotti L D 1975 *Phys. Rev.* B **12** 1778

[40] Pepperl G, Umlauf E, Meyer A and Keller J 1974 *Solid State Commun.* **14** 161

[41] Phillips N E and Fischer R A 2005 *J. Therm. Anal. Calorim.* **81** 631

[42] Maple M B, Ho P-C, Frederick N A, Zapf V S, Yuhasz W M, Bauer E D, Christianson A D and Lacerda A H 2003 *J. Phys.: Condens. Matter* **15** S2071

[43] Kabayashi M, Sato H, Sugawara H, Fujiwara H and Aoki Y 2005 *J. Phys. Soc. Japan* **74** 1690

[44] Izawa K, Nakajima Y, Goryo J, Matsuda Y, Osaki S, Sugawara H, Sato H, Thalmeier P and Maki K 2003 *Phys. Rev. Lett.* **90** 117001